

The First Integrated Optical Driver Chip for Fiber Optic Gyroscopes

Minh A. Tran, Jared C. Hulme, Tin Komljenovic, MJ Kennedy, Daniel J. Blumenthal and John E. Bowers
Department of Electrical and Computer Engineering
University of California, Santa Barbara, CA 93106, U.S.A.
E-mail: minhtran@ece.ucsb.edu

Abstract—We have designed and fabricated the first “integrated optical driver” chip for fiber gyroscopes on Si/III-V heterogeneous integration platform. The chip was successfully interrogated with a fiber coil to realize an open-loop IFOG.

Keywords—Integrated Optics, Gyroscopes, Silicon Photonics

I. MOTIVATION

An interferometric fiber optic gyroscope is formed by three essential components: a sensing coil, a set of active optical components and read-out electronics. Thanks to the ultra-low propagation loss in optic fibers, (IFOGs) was able to achieve extremely high sensitivity and has become a mature technology for inertial navigation systems [1]. However, its large footprint and power consumption have prevented FOGs from use in many growing fields such as robotics and automobiles. In recent years, there have been tremendous advances in making the sensing coil of the IFOG much more compact in size [2]. In addition, ultra-low loss waveguide has also been achieved on an integrated platform [3]. With those inventions, the size of the FOGs’ sensing part is going to be reduced significantly. However, the optical components that generate, modulate and detect the optical signal to drive the optical gyroscopes have not evolved comparably. Most modern IFOGs still use discrete optical components and these components are normally packaged with fiber pigtailed [1]. This not only results in a large footprint, but also degrades the gyroscope performance due to parasitic reflection and polarization misalignments at connection points.

In this paper, we present the design, fabrication and characterization of first fully integrated optical driver (IOD) chip that comprises all of the optical active components needed for optical gyroscopes (except the sensing coil). The chip is realized on Si-III-V heterogeneous platform with a volume smaller than 3.5 mm³.

II. CHIP DESIGN AND FABRICATION

A. Chip Layout

The schematic of the IOD chip is shown in Figure 1. The light source is a multi-mode Fabry-Perot laser which can be frequency modulated to reduce the coherence length and improve the gyroscope performance [4-5]. Three high speed photodiodes (~7 GHz bandwidth) on the circuit allow us not

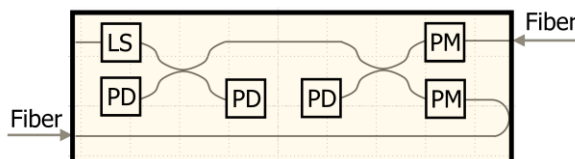


Figure 1: Schematic of the chip layout. LS: Light Source, PD: Photodiode, PM: Phase Modulator. Interfaces with single mode/polarization maintaining fibers are realized on two facets of the chip.

only to detect the Sagnac signal but also to monitor the output from the laser; through this monitor, corrections for the read-out of the gyroscope or stabilization of the laser power by an electronics feedback control loop are possible. The phase modulators have 2 GHz bandwidth and are laid out in a push-pull configuration to reduce the half-wave voltage. Two 3-dB splitters are based on the? adiabatic design to achieve ultra-broad bandwidth [6]. The two output waveguides are then inversely tapered to mode match with optical fibers.

B. Fabrication Process

The fabrication of the IOD chip includes a total of 22 processing steps with 17 lithographic mask layers. A simplified process flow with only the main steps is shown in Figure 2.

The fabrication started with Si waveguide etching on an SOI substrate that has 500 nm thick Si on top of a 1 μ m thick buried oxide layer. Waveguides were patterned on 248 nm DUV lithography and etched 200 nm with the SF6/C4F8 plasma based deep reactive-ion etching (RIE). The second lithography and etching were followed to define deeply etched waveguides and vertical outgassing channels. After the Si process, III-V epitaxial layers were bonded to the top using low temperature hydrophilic bonding process [7-8] to form active regions lasers, photodiodes and phase modulators. The III-V substrates were then removed by mechanical polishing and chemical wet etching before the p-mesas were dry etched down into the active region. The separate confined heterostructures (SCHs) and quantum wells were subsequently wet etched to n-type layers. Metal contacts were lifted-off to form n-metal layers. Oxide coverage deposition was followed to protect the waveguides and to form electrical isolation. Vias were opened by dry etch to allow for p-metal deposition. After

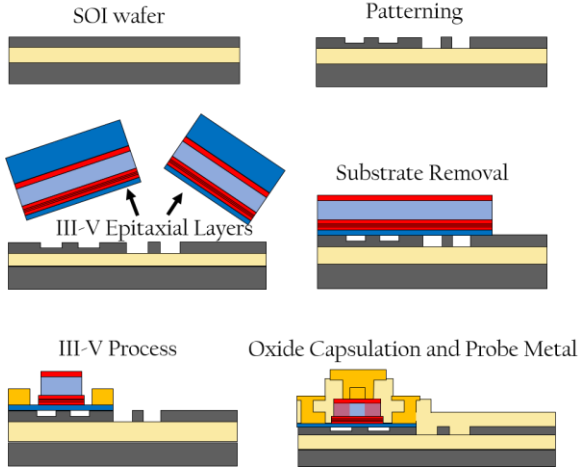


Figure 2: Fabrication process flow for the IOD chip on Si/III-V heterogeneous integration platform (from left to right, up to down).

proton implantation on two sides of the p-type mesas, Ti/Au stacks for probe pads were deposited. The fabrication was completed with dicing and Si facet polishing.

III. CHARACTERIZATION

Identical test structures for each component, fabricated in the same process with the IOD chip, allowed us to characterize them individually. The rotation measurement using the IFOG driven by the fabricated IOD chip will follow.

A. Individual Components

Optical spectrum of the Fabry-Perot laser when operating at

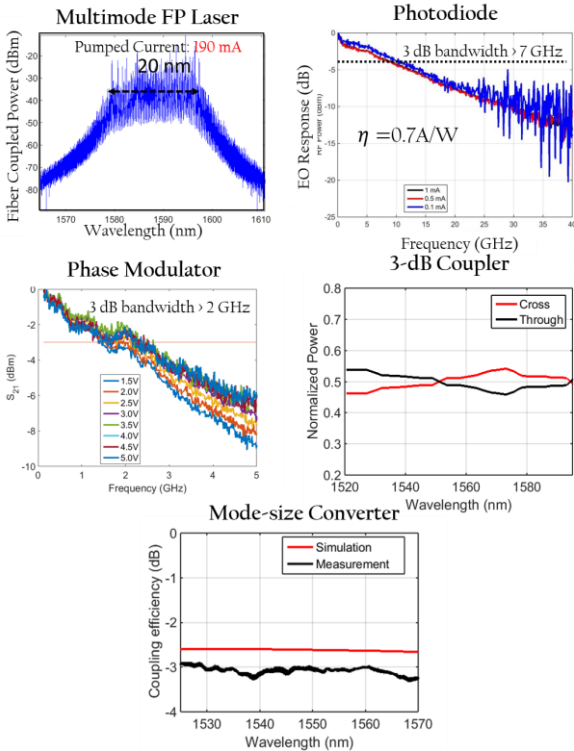


Figure 3: Performances of individual components of the IOD chip. All measurements were carried out at room temperature.

well above threshold is shown in the Figure 3. A multi-mode lasing across the 1578 – 1595 nm wavelength range was achieved with mode spacing of 0.07 nm corresponding to the designed cavity length of 4.5 mm formed by the two integrated loop mirrors.

The photodiode has a dark-current of 4 nA at -3 V and up to 15 nA at -6 V bias. The 3-dB bandwidth is larger than 6 GHz up to 1 mA photocurrent, with a responsivity of about 0.7 A/W.

The phase modulator has less than 1 dB insertion loss over C-band. The half-wave voltage for 500 μm long structure was measured to be 8.4 V. The modulator exhibited a 3 dB bandwidth of about 2 GHz at -2 V bias as shown in Figure 3.

The 2×2 adiabatic 3-dB coupler was characterized by using a rigorous method reported in [9]. The splitting ratios versus wavelength plot of the coupler is shown in the table. The splitter exhibited a flat wavelength response over the C-band. The normalized power splitting ratio over 75 nm wavelength range (1520 – 1595) was within 50±4.2%.

The mode size converter for waveguide-fiber coupler has averaged coupling loss of -3 dB over the C-band. The 0.3 dB discrepancy between measurement and simulation can be attributed to the propagation loss along the mode converter structure.

B. System Measurement

We tested the operation of the IOD on the setup shown in Figure 4. Two ends of a 180-meter long polarization maintaining (PM) fiber coil were connected to lensed PM fiber and coupled to the fabricated IOD and form an interferometric gyroscope. Using the small angle approximation, the scale factor is given by $I_0 R_{ESA} G J_1(\phi_b) \frac{8\pi L D}{\lambda c} \frac{\pi}{180}$ where $L = 180$ m is the length, $D = 0.2$ m is the diameter of the coil, $\lambda = 1.57$ μm is the mean-wavelength of the multimode laser, $I_0 = 8$ μA is the detected DC photocurrent, $R_{ESA} = 50$ Ω is the resistance of the ESA, $G = 10$ is the amplification of the RF amplifier and $J_1(\phi_b = 0.1)$ is the Bessel function of the first order at the phase modulation depth. The expected scale factor is calculated to be 6.70 μV/(°/s).

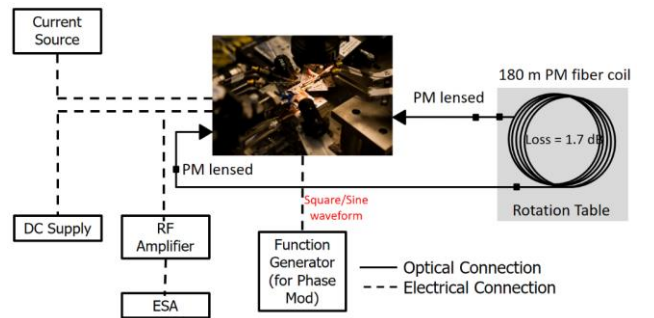


Figure 4: Gyroscope measurement setup

The chip and the 3-axis stages used to couple the light in and out of the chip were placed on an optical bench while the fiber coil was put on a separate rotation table. The coil was rotated back and forth in clockwise and counter-clockwise directions and the gyroscope output was read out by an electrical signal analyzer.

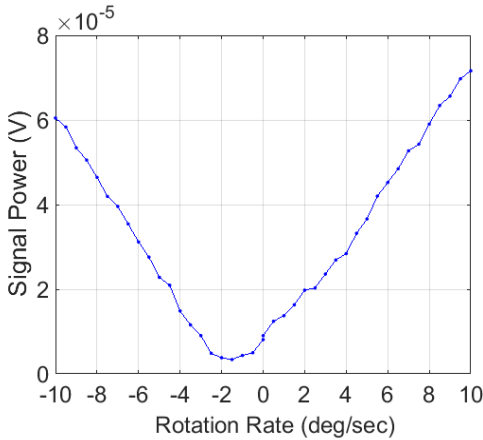


Figure 5: Gyroscope measurement result

The output signal voltage versus the rotation rate is plotted in Figure 5. It shows that the gyroscope output was linearly proportional to the applied rotation rate with a scale factor of $6.28 \mu\text{V}/(^{\circ}/\text{s})$. This agrees well with the calculated value above.

IV. DISCUSSION AND FUTURE WORK

We can observe that there is an offset of roughly $2^{\circ}/\text{s}$ in the rotation measurement. The possible causes for this offset could be electromagnetic interference (EMI) between components on the integrated circuit chip or phase error caused by residual amplitude modulation of the phase modulator [10]. Earth rotation and magnetic field induced nonreciprocal phase shift could also contribute a fraction to the offset. In practice, this offset can be calibrated out to correct the gyroscope's read-out.

For in-depth analysis of the sensitivity (*i.e.* angle random walk and bias instability) as well as all the noise processes limiting the performance of the IOD driven gyroscope system,

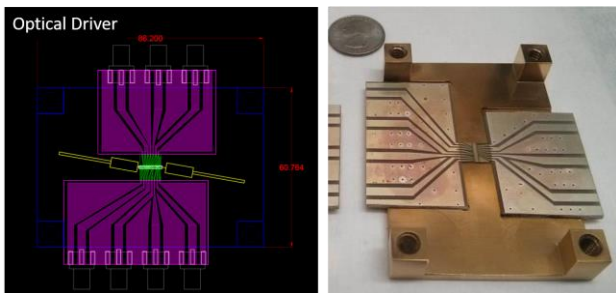


Figure 6: (Left) Schematic of the electrical and optical packaging for the IOD chip (Right) A photograph of the carrier.

we have to carry out time dependent measurements. However, due to the drift of the optical fiber-waveguides coupling, we were unable to do so. Permanent optical and electrical packaging is therefore needed.

Our packaging schematic is shown in figure 6, where electrical contacts are made by wire-bonds from the chip to AlN carrier and then to a PCB and optical lensed fiber holders come from an angle of 10° from two sides. Thermo-electric cooler can be installed underneath the copper carrier to stabilize the temperature of the chip in operation.

V. CONCLUSION

We have designed and fabricated an integrated optical driver chip for fiber optic gyroscopes. The rotation rate measurement using the chip and a PM fiber coil was successfully demonstrated for the first time.

ACKNOWLEDGMENT

The authors would like to thank Chao Xiang, Tony Huang, Sarat Gundaravapu, Taran Huffman, Michael Belt, and Dr. Robert Lutwak for fruitful discussions.

This research was developed with funding from the Defense Advanced Research Projects Agency (DARPA) within the Microsystems Technology Office Positioning, Navigation and Timing under Grant HR0011-14-C-0111. The views, opinions and/or findings expressed are those of the authors and should not be interpreted as representing the official views or policies of the Department of Defense or the U.S. Government.

REFERENCES

- [1] H. C. Lefevre, *The fiber-optic gyroscope* (Artech house, 2014).
- [2] R. A. Bergh, L. Arnesen and C. Herdman, "Fiber optic gyro development at Fibernetics," in *Fiber Optic Sensors and Applications XIII*, Proc. SPIE **9852** (2016).
- [3] J. F. Bauters, M. J. R. Heck, D. John, D. Dai, M.-C. Tien, J. S. Barton, A. Leinse, R. G. Heideman, D. J. Blumenthal and J. E. Bowers, "Ultra-low-loss high-aspect-ratio Si₃N₄," *Opt. Express* **19**(4) (2011).
- [4] Y. Shen, M. Tran, S. Srinivasan, J. Hulme, J. Peters, M. Belt, S. Gundavarapu, Y. Li, D. Blumenthal and J. Bowers, "Frequency modulated laser optical gyroscope," in *IEEE Photonics Conference* (2015).
- [5] T. Komljenovic, M. A. Tran, M. Belt, S. Gundavarapu, D. J. Blumenthal and J. E. Bowers, "Frequency modulated lasers for interferometric optical gyroscopes," *Opt. Lett.* **41**(8) (2016).
- [6] M. Tran, C. Zhang and J. Bowers, "A broadband optical switch based on adiabatic couplers," in *IEEE Photonics Conference* (2016).
- [7] H. Park, A. W. Fang, R. Jones, O. Cohen, O. Raday, M. N. Sysak, M. J. Paniccia and J. E. Bowers, "A hybrid AlGaInAs-silicon evanescent waveguide photodetector," *Opt. Express* **15**(10) (2007).
- [8] A. Fang, H. Park, O. Cohen, R. Jones, M. Paniccia and J. Bowers, "Electrically pumped hybrid AlGaInAs-silicon evanescent laser," *Opt. Express* **14**(20) (2006).
- [9] M. Tran, T. Komljenovic, J. Hulme, M. Davenport and J. Bowers, "A robust method for characterization of optical waveguides and couplers," *IEEE Photon. Technol. Lett.* **28**(14) (2016).
- [10] E. Kiesel, "Impact of modulation induced signal instabilities on fiber gyro performance," in *Fiber Optic and Laser Sensors V*, R. P. DePaula; E. Udd, eds., Proc. SPIE **838** (1987).